© 2014. Published by The Company of Biologists Ltd | Journal of Cell Science (2014) 127, 1550–1564 doi:10.1242/jcs.140855

RESEARCH ARTICLE

Transport and translation of MBP mRNA is regulated differently by distinct hnRNP proteins

Julie Torvund-Jensen, Jes Steengaard, Lasse Reimer, Linda B. Fihl and Lisbeth S. Laursen*

ABSTRACT

In the developing nervous system, abundant synthesis of myelin basic protein (MBP) in oligodendrocytes is required for the formation of compact myelin sheaths around axons. The MBP mRNA is known to be transported into the processes of oligodendrocytes. However, knowledge of the regulatory mechanisms that ensure the tight temporal and spatial control of MBP translation within these processes is limited. Here, we have identified novel regions within the 3′-UTR of the MBP mRNA that are responsible for the regulation of its translation, and we have demonstrated that each of the mRNA-binding proteins heterogeneous nuclear ribonucleoprotein (hnRNP)-A2, hnRNP-K and hnRNP-E1 serve distinct functions to regulate controlled and localized protein synthesis. hnRNP-A2 is responsible for mRNA transport, not for translational inhibition. By contrast, hnRNP-K and hnRNP-E1 play opposing roles in the translational regulation of MBP mRNA. We have identified shared binding sites within the 3′-UTR, and show that translation is promoted by the exchange of inhibitory hnRNP-E1 for stimulatory hnRNP-K. We further show that this molecular switch in the MBP messenger RNA-ribonucleoprotein (mRNP) complex, which regulates the synthesis of MBP, is important for the normal growth and extension of myelin sheets.

KEY WORDS: Cellular asymmetry, Local translation, RNA-binding proteins, Oligodendrocyte, Myelin basic protein

INTRODUCTION

The asymmetric distribution of proteins within cells is essential for many different processes during development, including cell fate determination, cell migration and the formation of neuronal networks. One mechanism by which cellular asymmetry can be established is through mRNA transport combined with regulated local protein synthesis (St Johnston, 2005; Pratt and Mowry, 2013). The spatial and temporal regulation of the translation of transported mRNA is mediated by the formation of ribonucleoprotein (RNP) particles, in which complexes of trans-acting factors interact with cis-regulatory elements within the mRNA (Gebauer et al., 2012). The complexity of these regulatory mechanisms has become evident from recent studies of different systems, which have revealed the presence of several regulatory elements within the 3′-UTR region of tightly regulated mRNAs (Xing and Bassell, 2013). However, knowledge of the dynamics of translational regulation by the RNA binding proteins in RNP complexes is limited.

In the central nervous system, the formation of myelin sheaths around axons by oligodendrocytes represents a unique example of the establishment of cellular asymmetry, with an uneven distribution of myelin proteins within the oligodendrocyte. Specifically, myelin basic protein (MBP), one of the major myelin proteins, is confined to the myelin sheaths in the myelinating oligodendrocytes, where it is essential for the compaction of myelin sheets (Readhead et al., 1987). A specific MBP:lipid ratio is required to induce membrane fusions (Min et al., 2009), and, furthermore, the onset of MBP synthesis has been suggested to control the segregation of other myelin membrane proteins between compacted and non-compacted regions of the myelin sheath (Aggarwal et al., 2011; Aggarwal et al., 2013). These data support a hypothesis predicting that tight spatial and temporal control of MBP synthesis is required for the normal formation of myelin sheaths. In fact, MBP mRNA is known to be transported into the oligodendrocyte processes (Trapp et al., 1987; Ainger et al., 1993), and, based on the fast incorporation of newly synthesized MBP into myelin compared with another major myelin protein, PLP (Colman et al., 1982), MBP mRNA has been speculated to be translated under local regulation.

The transport of MBP mRNA was initially shown to depend on two regions within the 3′-UTR, the 21-nucleotide RNA trafficking sequence (RTS), which is required for transport from the cell body into the oligodendrocyte processes, and a second longer stretch, the RNA localization element (RLR), which is required for final transport into the myelin sheet (Ainger et al., 1997). The RTS includes the binding site for heterogeneous nuclear ribonucleoprotein (hnRNP)-A2 (Hoek et al., 1998; Munro et al., 1999), a protein that is known to be necessary for transport of the mRNA (Kwon et al., 1999; Laursen et al., 2011). More recent experiments have identified additional proteins associated with hnRNP-A2 or the RTS. These include hnRNP-F (White et al., 2011), CBF-A (Raju et al., 2008), hnRNP-E1 (also known as PCBP1) (Kosturko et al., 2006) and TOG (Kosturko et al., 2005). In contrast to the RTS, trans-acting factors associated with the RLR have not been identified. Furthermore, it is not clear to what extent the same proteins might be involved in both transport and translational regulation of the mRNA. Interestingly, from experiments based on truncated mRNA molecules, it has been proposed that hnRNP-E1 regulates translation through its interaction with hnRNP-A2 (Kosturko et al., 2006).

Following transport of the RNP particles, the synthesis of MBP is suggested to be stimulated by signals that originate at the interface between the oligodendrocyte processes and the axons. Specifically, recent findings provide possible links between extracellular mechanisms and regulation at the level of mRNA

Department of Molecular Biology and Genetics, Aarhus University, Gustav Wieds Vej 10C, 8000 Aarhus C, Denmark.

*Author for correspondence (ll@mb.au.dk)

Received 19 August 2013; Accepted 23 January 2014

Journal of Cell Science

Journal of Cell Science (2014) 127, 1550–1564 doi:10.1242/jcs.140855

translation. Neuronal activity stimulates MBP synthesis by a mechanism that involves upregulation of the adhesion molecule L1 on the axonal surface and depends on the Src family kinase Fyn, which is present in the oligodendrocytes (Wake et al., 2011). Other studies have shown that L1 induces Fyn activation (White et al., 2008; Laursen et al., 2009), causing the phosphorylation of hnRNP-A2 and the release of both hnRNP-A2 and hnRNP-E1 from mRNA transport granules (White et al., 2008). In addition, integrin signaling causes Fyn activation (Colognato et al., 2004; Laursen et al., 2009), and stimulates MBP synthesis through interaction with another mRNA-binding protein, hnRNP-K, which is also known to bind to the MBP mRNA (Laursen et al., 2011).

These reports indicate that hnRNP-E1 and hnRNP-K, in addition to hnRNP-A2, are crucial trans-acting factors that regulate the transport and/or translation of MBP mRNA. However, the mechanistic details of how they work together are not known. Here, we aim to define regulatory regions within the mRNA, to delineate how the hnRNPs interact with these regions, to assess the regulatory potential of the individual factors, and to analyze the consequences of a disturbed balance between the regulatory proteins on myelin sheet formation.

RESULTS

Identification of translational regulatory regions within the 3′-UTR of MBP mRNA

To identify regions within the ~1500 nucleotide 3′-UTR of MBP mRNA that are important for translational regulation, we replaced the MBP coding sequence with sequence encoding EGFP, and analyzed the expression of variants with progressively truncated 3′-UTRs (Fig. 1A) in Oli-neu cells (Fig. 1B). By using this approach, we found that two regions of the MBP mRNA (nucleotides 640–810 and 963–1500) seemed to be involved in translational inhibition (Fig. 1B). The presence of inhibitory elements within these regions was further confirmed by their ability to inhibit translation in the absence of the flanking regions. The region between nucleotides 963 and 1500 showed the most efficient inhibition (supplementary material Fig. S1C,D). Interestingly, these two regions partially overlapped with two regions that were shown previously to be important for transport of the mRNA into the processes of the oligodendrocyte and further into the myelin sheets (Ainger et al., 1997) (Fig. 1C). The first of the identified regions (640–810) includes the RTS, which contains a binding site for hnRNP-A2 (termed the hnRNP-A2 response element or A2RE) (Munro et al., 1999). Proteins potentially binding to the second regulatory region are currently unknown.

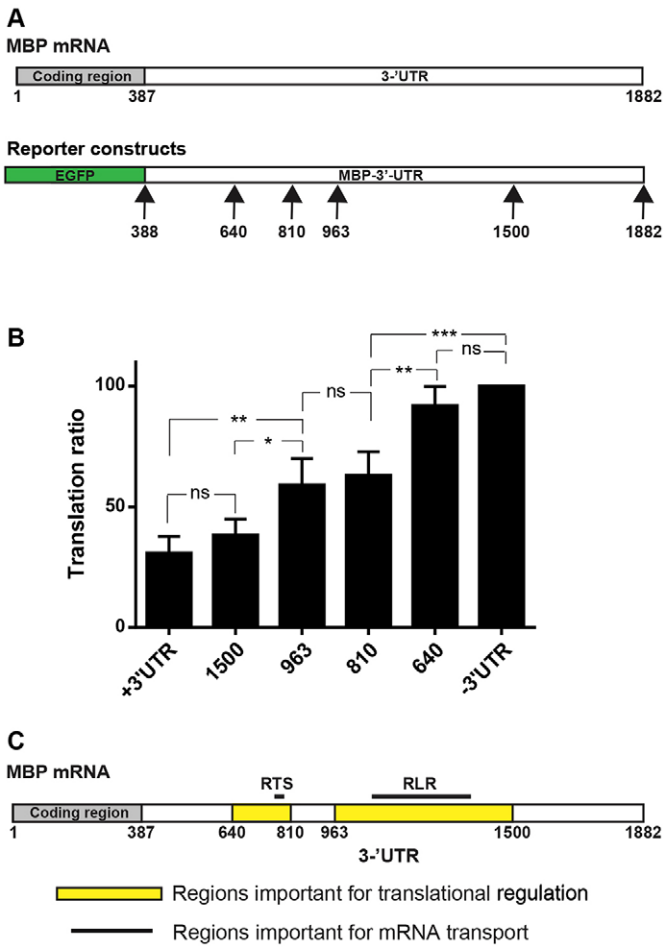

Fig. 1. Two regions within the 3′-UTR of MBP mRNA are required for translational inhibition. (A) Diagram of the coding region (nucleotides 1–387) and the 3′-UTR (nucleotides 388–1882) of the myelin basic protein (MBP) mRNA. Reporter constructs, in which the 3′-UTR sequence is progressively truncated and the MBP coding sequence is replaced with EGFP cDNA, are indicated below. None of the mRNA variants showed decreased stability (supplementary material Fig. S1B). (B) Flow cytometry analysis of Oli-neu cells co-transfected with the reporter constructs and a DsRed-expressing vector as a control for transfection efficiency. The relative EGFP expression, displayed as the translation ratio, was calculated as described in the Materials and Methods section. Data represent the mean±s.d. from at least three independent experiments. *$P<0.05$; **$P<0.01$; ***$P<0.001$; ns, non-significant (one-way ANOVA followed by Tukey's multiple comparison). (C) The identified regions are depicted relative to the two regions previously shown to be important for mRNA transport (RTS and RLR) (Ainger et al., 1997).

Mapping of the hnRNP-K-binding site in the 3′-UTR of MBP mRNA

We have recently found that hnRNP-K binds to MBP mRNA and is associated with hnRNP-A2 in an mRNA-dependent manner (Laursen et al., 2011). Previous results, based on SELEX experiments (Thisted et al., 2001) and crystal structure data (Backe et al., 2005), suggest that $UC_{3–4}$(U/A) is the minimal consensus sequence required for the binding of hnRNP-K. We therefore generated a series of RNA probes containing all 12 potential binding sites within the MBP mRNA (Fig. 2A), and assessed their binding to recombinantly expressed and purified hnRNP-K in gel-shift assays. In the initial screen, seven of the probes showed possible binding to hnRNP-K (Fig. 2B). Further analysis using decreasing concentrations of hnRNP-K confirmed binding of three probes – P539–574, P799–838 and P1455–1493 (Fig. 2C). Interestingly, the binding site of probe P1455–1493 was located within the second sequence stretch (963–1550) that we identified as being important for translational inhibition. Hence, hnRNP-A2 and hnRNP-K each binds within one of the two different regulatory regions (Fig. 1C), leading us to speculate that hnRNP-A2 and hnRNP-K function together to prevent translation during mRNA transport.

hnRNP-A2 and hnRNP-K do not inhibit MBP mRNA translation

To address this question, primary oligodendrocyte precursors were treated with siRNA to analyze the effect of knockdown of hnRNP-K or hnRNP-A2 on MBP synthesis in maturing cells.

Journal of Cell Science (2014) 127, 1550–1564 doi:10.1242/jcs.140855

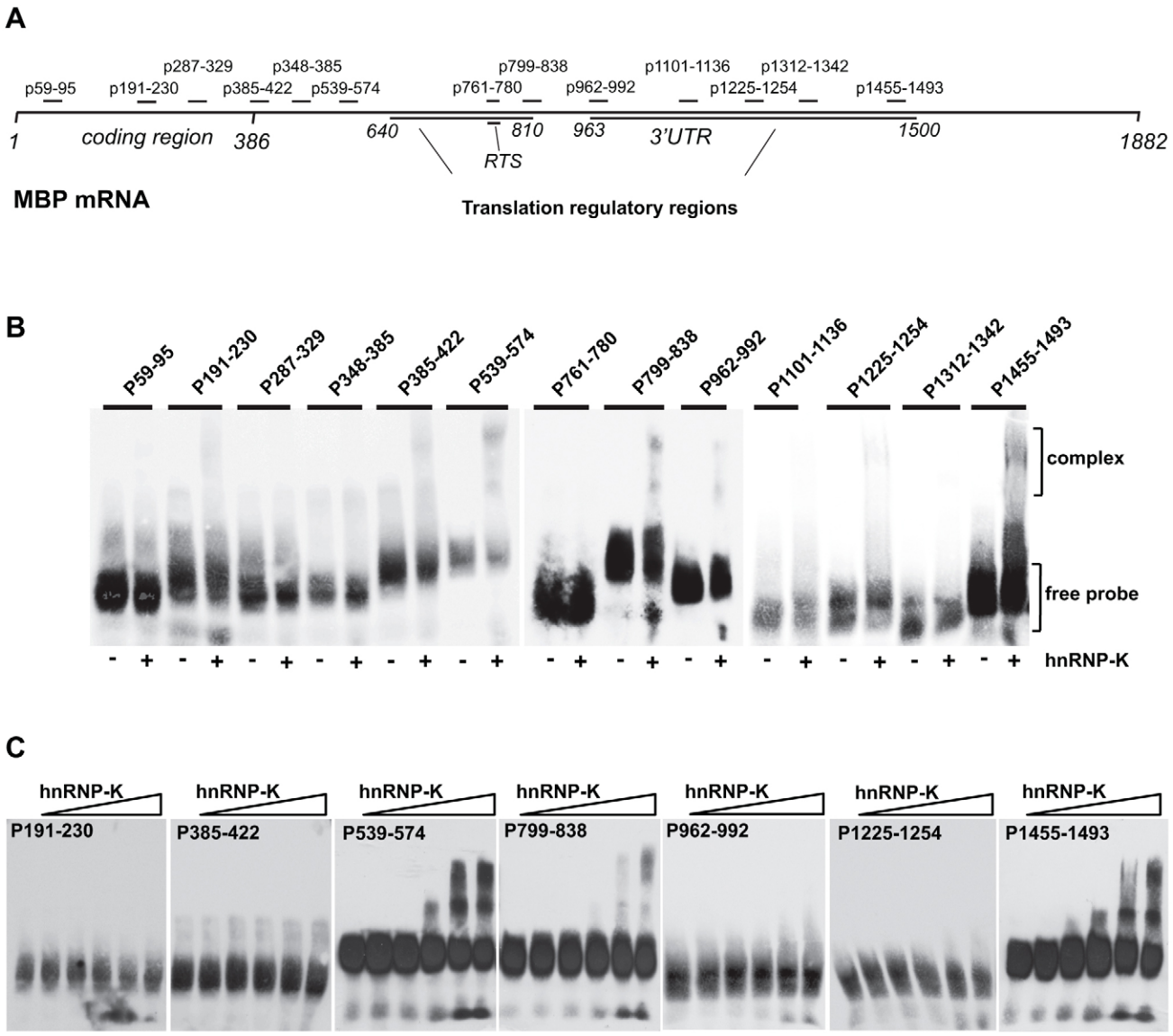

Fig. 2. Identification of binding sites for hnRNP-K within the MBP mRNA. (A) Localization within the MBP mRNA of 12 RNA probes, synthesized and used for binding analysis. All probes are located in sequence stretches containing the $UC_{3–4}$(U/A) consensus motif (Thisted et al., 2001). In addition, a probe containing the hnRNP-A2-binding site, A2RE (p761–780), was used as a negative control. Probe sequences are specified in supplementary material Fig. S2A. (B) EMSA performed with 3′-end-biotinylated RNA probes (0.125 μM). The identity of the probes is indicated above the lanes. The absence (−) or presence (+) of purified recombinant hnRNP-K (1.2 μM) is indicated below the gel images. (C) Selected probes were analyzed as in B but with increasing concentration (150 nM–1.0 μM) of purified recombinant hnRNP-K. The EMSA results shown in B and C are representative of at least three independent experiments.

As expected, individual knockdown of hnRNP-K or hnRNP-A2 caused a reduction in MBP synthesis, but, surprisingly, the combined knockdown also caused a reduction in MBP synthesis compared with cells treated with control siRNA or non-treated cells (Fig. 3A). By using immunocytochemistry, MBP expression was further analyzed at the level of individual cells (Fig. 3B). The number of mature [myelin-associated glycoprotein (MAG)-positive] cells was constant (Fig. 3C), but the number of MBP-positive cells showed a marked reduction (Fig. 3D) following knockdown of hnRNP-K and hnRNP-A2, either alone or in combination. Importantly, no differences in the morphology of the MAG-positive cells were observed (Fig. 3B,E), confirming that the reduced expression of MBP was not a consequence of a general delay in differentiation of the oligodendrocyte precursors into mature oligodendrocytes. Furthermore, the level of MBP mRNA did not differ between the control and knockdown cells (supplementary material Fig. S3A), excluding the possibility that the reduced expression was a result of a decreased stability of the MBP mRNA.

Interestingly, both hnRNP-A2 (Kosturko et al., 2006; White et al., 2008) and hnRNP-K (Laursen et al., 2011) have been assumed previously to play a dual role in mRNA transport and inhibition of translation during transport. To confirm our findings that hnRNP-A2 binding does not mediate translational inhibition, we assessed the effect of deleting the hnRNP-A2-binding site in the 3′-UTR or replacing a single nucleotide, shown previously to abolish hnRNP-A2 binding (Munro et al., 1999). In agreement with our findings reported above, neither of the variants carrying

Journal of Cell Science (2014) 127, 1550–1564 doi:10.1242/jcs.140855

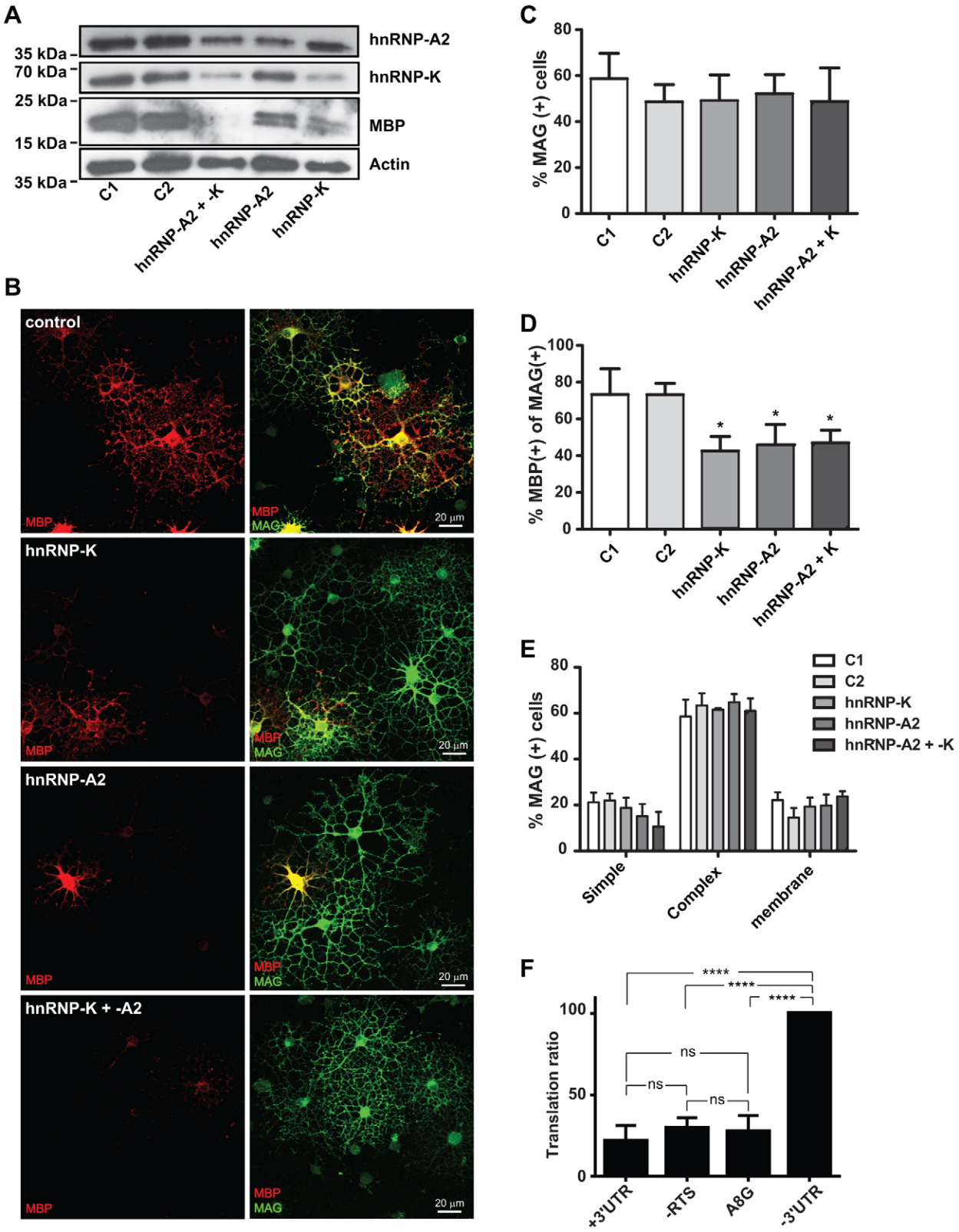

Fig. 3. See next page for legend.

these mutations caused an increase in translational activity (Fig. 3F). We therefore conclude that neither hnRNP-A2 nor hnRNP-K is required to maintain translational silencing of the mRNA during transport.

MBP mRNA translation is inhibited by hnRNP-E1

It has previously been shown that hnRNP-E1 interacts with hnRNP-A2, and *in vitro* translation experiments using a minimal construct containing only the hnRNP-A2-binding site of the 3′-UTR suggest

Journal of Cell Science

Journal of Cell Science (2014) 127, 1550–1564 doi:10.1242/jcs.140855

Fig. 3. hnRNP-K and hnRNP-A2 are not involved in translational inhibition. (A) Western blotting for hnRNP-A2, hnRNP-K and MBP expression in oligodendrocytes generated from oligodendrocyte precursors following mock transfection (C1), or following transfection with non-targeting siRNA (C2) or siRNA targeting hnRNP-A2, hnRNP-K or both hnRNP-A2 and hnRNP-K, as indicated. Actin was used as a loading control. Note that knockdown of hnRNP-A2 and hnRNP-K, either individually or in combination, caused reduced MBP expression. (B) Immunocytochemistry for MBP (red) in oligodendrocytes generated from oligodendrocyte precursors that were transfected with non-targeting siRNA (control) or transfected with siRNA targeting either hnRNP-A2 or hnRNP-K, or both hnRNP-A2 and hnRNP-K, as indicated. Cells are also stained for MAG (green), a marker of mature oligodendrocytes. (C) The percentage of mature (MAG-positive) cells. Note that knockdown of either hnRNP-A2 or hnRNP-K, or the combined knockdown, did not have any effect on the percentage of mature cells. (D) The percentage of mature cells, which are positive for MBP. Note that knockdown of either hnRNP-A2 or hnRNP-K, or the combined knockdown, reduced the percentage of MBP-positive cells. (E) The morphology of the mature cells was scored as 'simple', 'complex' or 'membrane'. The percentage of cells in each category is shown. Note that knockdown of neither hnRNP-A2 or hnRNP-K, nor the combined knockdown, had any effect on the morphology of the cells. (F) Using the EGFP reporter assay (Fig. 1), the effect on translational inhibition of a deletion (-RTS) or a disrupting point mutation (A8G) in the hnRNP-A2 binding site of the 3′-UTR of the MBP mRNA was analyzed. Note that neither the removal of the entire RTS sequence nor a mutation in the hnRNP-A2-binding site had any effect on the translational inhibition exerted by the 3′-UTR. (C–F) The cells were analyzed after 2.5 days in culture, and the data represent the mean±s.d. of at least three independent experiments. (C–E) For each independent experiment, ten randomly selected pictures from each of two coverslips were analyzed (~200 cells per coverslip). *$P<0.05$; ****$P<0.0001$; ns, non-significant (one-way ANOVA followed by Tukey's multiple comparison test).

that hnRNP-E1 inhibits translation in a manner that is dependent on hnRNP-A2 (Kosturko et al., 2006). However, because we find that the binding of hnRNP-A2 is not required for inhibition, we assessed the role of hnRNP-E1 in primary oligodendrocytes.

Overexpression of hnRNP-E1 reduced the number of oligodendrocytes expressing MBP (Fig. 4). After 2 days of differentiation, we observed a reduction in the percentage of O4-positive (maturing) oligodendrocytes synthesizing MBP following transfection with hnRNP-E1 cDNA (Fig. 4A,B). A similar reduction was observed at day 3 (Fig. 4C), and the cell morphology was still not significantly changed (Fig. 4D,E). Taken together, these experiments suggest that hnRNP-E1 inhibits MBP expression.

Conversely, siRNA-mediated knockdown of hnRNP-E1 induced premature MBP expression. Following 1.5 days of differentiation, an increased percentage of mature (MAG-positive) cells were also found to be MBP-positive (Fig. 4F,G). These cells showed normal branching morphology (Fig. 4F,H). At day 2.5, no significant difference in MBP expression was observed between cells treated with control siRNA and siRNA targeting hnRNP-E1 (Fig. 4I–K). Interestingly, at day 2.5, marked changes in the morphology of the cells were observed following hnRNP-E1 knockdown (Fig. 4I,L), with an increased number of cells failing to extend long branched processes that are required for the formation of a complex network. Premature translation of MBP therefore seems to have a general impact on the morphological differentiation of the cells. However, we cannot exclude that this is caused in part by other functions of hnRNP-E1.

hnRNP-E1 binds MBP mRNA independently of hnRNP-A2

Based on the results reported above, we speculated that hnRNP-E1 inhibits translation in oligodendrocytes independently of hnRNP-A2. We first asked whether hnRNP-E1 is associated with the MBP mRNA. Immunoprecipitation of hnRNP-E1 followed by quantitative RT-PCR clearly demonstrated this association (Fig. 5A). Therefore, we further asked whether hnRNP-E1 interacts directly with the MBP mRNA. In contrast to hnRNP-K, previous experiments do not define a minimal consensus sequence for the binding of hnRNP-E1 to mRNA. However, hnRNP-E1 has a preference for binding to poly-cytosine (C)-rich regions (Dejgaard and Leffers, 1996), and structural data shows that, similar to hnRNP-K, a minimum of three cytosine nucleotides is required for the binding to one of the three K homology (KH) domains of hnRNP-E1 (Yoga et al., 2012). hnRNP-E1 binds to differentiation control elements (DICEs) (Ostareck et al., 1997), and the 5′-end of the DICE, which contains only two stretches of poly-C, is sufficient for binding to hnRNP-E1 (Reimann et al., 2002). However, the binding affinity is significantly increased by the presence of multiple DICE repeats (Reimann et al., 2002). Furthermore, a comparison of other mRNA sequences known to bind hnRNP-E1 indicates that the presence of two to three C-rich stretches is required for binding (Holcik and Liebhaber, 1997). We therefore suggest that [(A/U)$C_{3–5}$(A/U)-n_x-(A/U)$C_{3–5}$(A/U)] represents a minimum consensus motif for the binding of hnRNP-E1 to mRNA.

In the MBP mRNA, we identified seven potential hnRNP-E1-binding sites (Fig. 5B) that conformed to the minimum consensus motif proposed. We assessed the binding of recombinantly expressed and purified hnRNP-E1 to RNA probes spanning the seven potential binding sites and to a negative control probe containing the hnRNP-A2-binding site (Fig. 5B). We identified three candidate probes in the initial screen (Fig. 5C), and further analysis with decreasing concentrations of hnRNP-E1 demonstrated two strong binders, probes P539–574 and P1455–1493 (Fig. 5D). Surprisingly, comparison with the mapping of hnRNP-K binding (Fig. 2) revealed that these two binding sites of hnRNP-E1 overlapped with two of the three hnRNP-K-binding sites (Fig. 5E). To test whether hnRNP-K and hnRNP-E1 could, in fact, compete for binding to the MBP mRNA, EMSA supershift assays were carried out. In this setup, the presence of hnRNP-K reduced the binding of hnRNP-E1 to P539–574 but not to P1455–1493 (supplementary material Fig. S3B,C). Further analysis with full-length *in-vitro*-transcribed MBP mRNA and purified hnRNP-E1 and -K showed that excess hnRNP-K reduced the amount of mRNA associated with hnRNP-E1 (Fig. 5F). This immediately suggested that a dynamic regulation of translation might involve competition between hnRNP-K and hnRNP-E1 for binding to the 3′-UTR of the MBP mRNA.

hnRNP-K and hnRNP-E1 have opposite roles in the regulation of MBP mRNA translation

To test whether hnRNP-K and hnRNP-E1 can bind to the MBP mRNA at the same time, immunoprecipitation from lysates of mature primary oligodendrocytes was carried out for both proteins. Precipitation of hnRNP-K did not co-precipitate hnRNP-E1, and no hnRNP-K was detected in hnRNP-E1 precipitates (Fig. 6A). However, hnRNP-A2 precipitated with both hnRNP-K and hnRNP-E1. Interestingly, the precipitation of hnRNP-A2 with hnRNP-K was abolished by RNase treatment, whereas precipitation of hnRNP-A2 with hnRNP-E1 was not RNA dependent (Fig. 6A), demonstrating a direct interaction between hnRNP-E1 and hnRNP-A2. We therefore suggest that, at a given stage of mRNA transport, only hnRNP-E1 or hnRNP-K can be associated with the MBP mRNA. Their different modes of

Journal of Cell Science (2014) 127, 1550–1564 doi:10.1242/jcs.140855

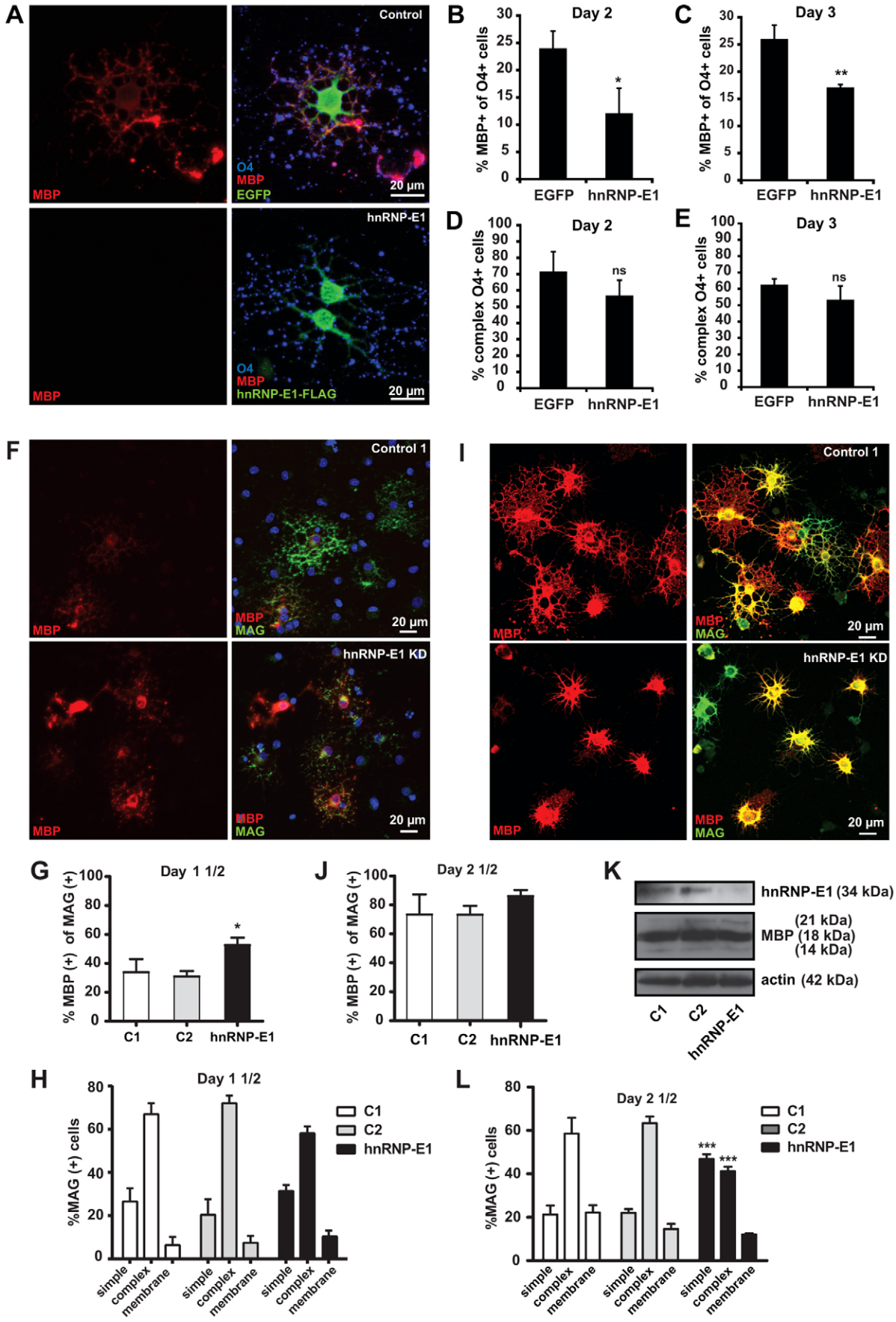

Fig. 4. See next page for legend.

Fig. 4. MBP expression is regulated by hnRNP-E1.
(A) Immunocytochemistry of oligodendrocytes generated from oligodendrocyte precursors that were transfected with EGFP (green) or hnRNP-E1-FLAG (green), and were stained 2 days after their transfer to differentiation medium. The cells were also stained for MBP (red) and O4 (blue), a marker of maturing oligodendrocytes. The percentage of O4-positive cells that were also positive for MBP at day 2 (B) and day 3 (C), and the percentage of oligodendrocytes showing complex branching morphology at day 2 (D) and day 3 (E), are shown. The data represent the mean±s.d. of three independent experiments, with at least 130 transfected cells analyzed in each independent experiment. *$P<0.05$; **$P<0.01$; ns, non-significant (Student's *t*-test). (F–L) Oligodendrocyte precursors were mock transfected (C1), or transfected with non-targeting siRNA (C2) or siRNA targeting hnRNP-E1. (F) At 1.5 days after transfer to differentiation medium, the cells were stained for MBP (red) or MAG (green), a marker of mature oligodendrocytes. (G) The percentage of MBP-positive mature oligodendrocytes is shown. (H) The distribution of the mature cells between 'simple', 'complex' or 'membrane' morphology. A similar experiment was carried out in which the cells were stained and analyzed at 2.5 days after transfer to differentiation medium (I,J,L). In this experiment, the expression of hnRNP-E1 and MBP was assessed by western blotting using actin as a loading control (K). The percentage of MAG-positive cells at day 1.5 and 2.5 were ~25% and 50%, respectively. The data show the mean±s.d. of three independent experiments. For each experiment, 10 randomly selected pictures from each of two coverslips were analyzed (~200 cells per coverslip). *$P<0.05$; **$P<0.01$; ***$P<0.001$; ns, non-significant (one-way ANOVA followed by Tukey's multiple comparison test).

association with hnRNP-A2 might cause the entire RNP complex to be reorganized upon exchange of hnRNP-E1 for hnRNP-K.

Differential synthesis of hnRNP-E1 and hnRNP-K during the differentiation of oligodendrocyte precursors into mature cells potentially determines the occupancy of an mRNA-binding site that is common to these two proteins. However, western blotting of lysates taken at time-points during which MBP was dramatically increased showed that the expression of neither hnRNP-E1 nor hnRNP-K was changed over this time period (Fig. 6B). Therefore, to test the hypothesis that altered local availability of hnRNP-E1 and hnRNP-K might determine the extent to which they bind to the mRNA, their subcellular localization was assessed both before and after the initiation of MBP expression (Fig. 6C). In oligodendrocytes with a complex branching morphology, but which did not yet show any MBP expression, hnRNP-E1 was present throughout the cells, with the highest concentration in the cell body. Following the onset of MBP synthesis, hnRNP-E1 localized primarily to the cell body and primary processes, with very low levels in the developing MBP-positive myelin sheets. This distribution contrasted with that of hnRNP-K, which, in cells not yet expressing MBP, was mainly confined to the nucleus. Following the onset of MBP synthesis, hnRNP-K also localized in granules of the developing myelin sheets. In these areas, very limited colocalization of hnRNP-E1 and hnRNP-K was observed (Fig. 6C, insert).

To test the possibility that the balance between hnRNP-E1 and hnRNP-K differentially regulates MBP translation, the level of MBP protein synthesis in the absence and presence of hnRNP-K and hnRNP-E1 was analyzed in an *in vitro* translation system. We found that hnRNP-K increased MBP translation, and that this was counteracted by hnRNP-E1 (Fig. 7A). The ability of increased levels of hnRNP-K to drive cells towards MBP expression was then tested by overexpression in primary oligodendrocytes. We observed that a larger fraction of the hnRNP-K-overexpressing cells expressed MBP at day 2 (Fig. 7C,D). This effect was maintained at day 3 (Fig. 7E). Importantly, no significant change in morphology was observed in the hnRNP-K-overexpressing cells compared with control cells (Fig. 7F,G), suggesting that increased availability of hnRNP-K is able to overcome the translational inhibition of the MBP mRNA in a spatially controlled manner. Taken together, the balance between hnRNP-E1 and hnRNP-K therefore represents a molecular switch that temporally and spatially controls translation of the MBP mRNA.

Finally, we assessed the consequences of disturbing this balance on oligodendrocyte functionality (Fig. 8). Whereas knockdown of hnRNP-E1 resulted in rudimentary cells with very short processes, knockdown of hnRNP-K caused the oligodendrocytes to assume a phenotype in which the processes and myelin sheets were extended to cover a larger surface area (Fig. 8A–C). This result implies that the timing and spatial control of MBP expression might impact on the extension of processes required for myelination, highlighting the importance of accurate translational control.

DISCUSSION

Here, we identify stretches within the 3′-UTR of the MBP mRNA that are required for trans-acting factors to negatively affect translation (Fig. 1). The first of these inhibitory regions (nucleotides 640–810) contains the RTS, which is necessary for transport of the mRNA into the oligodendrocyte processes. The hnRNP-A2 binding site is located within the RTS (Hoek et al., 1998), and knockdown of hnRNP-A2 abrogates mRNA transport (Kwon et al., 1999; Munro et al., 1999; Laursen et al., 2011). However, neither siRNA-mediated knockdown of hnRNP-A2 (either alone or in combination with hnRNP-K) nor deletion of the RTS leads to premature translation of the MBP mRNA (Fig. 3). Therefore, unlike previous suggestions, hnRNP-A2 is not required for the inhibition of translation, but rather serves to mediate transport of the mRNA. Other trans-acting factors are therefore likely to be responsible for the inhibitory effect of this region. One candidate is the short non-coding RNA sncRNA175, which was recently identified as a negative regulator of MBP mRNA translation (Bauer et al., 2012). Further analysis of how factors associated with this region work together with factors associated with the second translational regulatory region will be required to fully understand the control of MBP mRNA translation.

We further identify three binding sites for hnRNP-K in the MBP mRNA, which conform to the consensus motif UC_{3-4}(U/A), (Fig. 2). Two of these hnRNP-K-binding sites are shared with hnRNP-E1. One of the shared binding sites (within nucleotides 539–574) is not conserved between rodents and human, but another potential binding site is present ~40 nucleotides upstream in the human sequence. By contrast, the other site (within nucleotides 1455–1493), which is located in the second inhibitory region (nucleotides 964–1500) (Fig. 1), is conserved between rat, mouse and human. It is therefore very interesting that knockdown of hnRNP-K results in decreased expression of MBP (Fig. 3), and that hnRNP-K overexpression increased the number of MBP-expressing cells (Fig. 7). By contrast, knockdown of hnRNP-E1 causes premature MBP expression (Fig. 4), and hnRNP-E1 overexpression delays the expression of MBP (Fig. 4). No interaction between hnRNP-E1 and hnRNP-K was observed under conditions where both proteins interact with hnRNP-A2, and the two proteins did not colocalize in RNA granules of oligodendrocytes (Fig. 6). In addition, we demonstrate that hnRNP-K is able to compete with hnRNP-E1 for binding to MBP mRNA (Fig. 5F), and that the two proteins also have counteracting effects on translation *in vitro* (Fig. 7A). Our

Journal of Cell Science (2014) 127, 1550–1564 doi:10.1242/jcs.140855

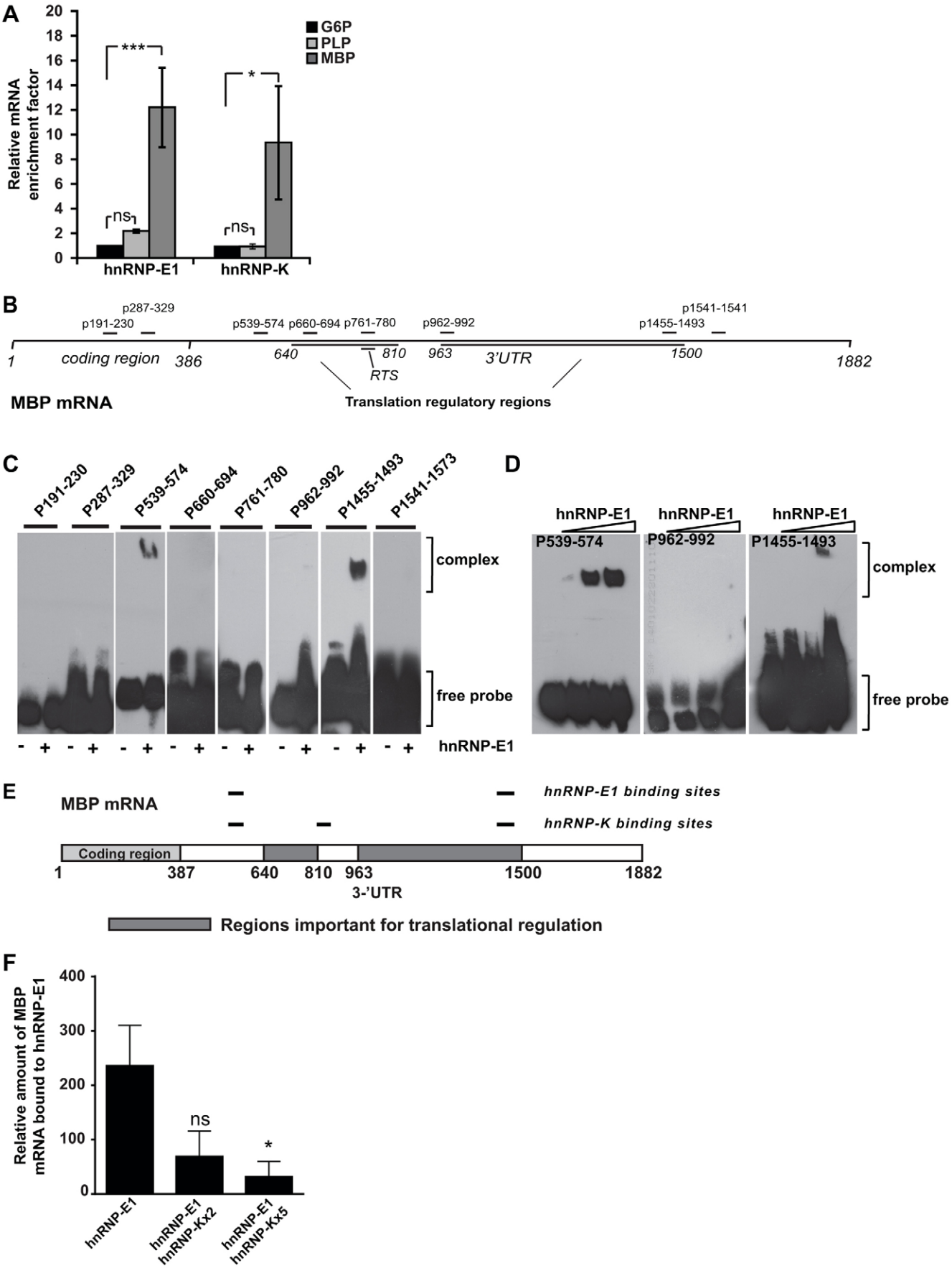

Fig. 5. See next page for legend.

Journal of Cell Science (2014) 127, 1550–1564 doi:10.1242/jcs.140855

Fig. 5. hnRNP-E1 binds directly to MBP mRNA and competes with hnRNP-K for binding. (A) RNA-immunoprecipitation from lysates of oligodendrocyte precursors that were differentiated for 4 days, using antibodies against hnRNP-E1 or hnRNP-K, or control IgG. The amount of co-precipitated MBP, PLP or G6PDH mRNA was quantified by using qRT-PCR, and the enrichment was calculated relative to the amount of mRNA obtained by immunoprecipitation with control IgG antibody. Data show the mean±s.d. of three independent experiments. Statistical significance was analyzed by one-way ANOVA followed by Tukey's multiple comparison test. (B) The localization of seven RNA probes within the MBP mRNA that were used for binding analysis. All probes are located in sequence stretches containing the $[(A/U)C_{3–5}(A/U)\text{-}n_x\text{-}(A/U)C_{3–5}(A/U)]$ motif. A probe containing the hnRNP-A2-binding site, A2RE (p761–780), was used as a negative control. Probe sequences are specified in supplementary material Fig. S2B. (C) EMSA carried out with 3′-end-biotinylated RNA probes (0.125 μM). Probe identities are shown above the images, and the absence (−) or presence (+) of purified recombinant hnRNP-E1 (1.2 μM) is indicated below the gel images. (D) Selected probes were analyzed as in B but with increasing concentration (150 nM–1.0 μM) of purified recombinant hnRNP-E1. The images shown in C and D are representative of at least three independent experiments. (E) Schematic representation of the identified binding sites of hnRNP-E1 and hnRNP-K within the MBP mRNA. (F) *In vitro* transcribed MBP mRNA was preincubated with recombinant purified hnRNP-E1, followed by competition by hnRNP-K that was present at twofold or fivefold molar excess, as indicated. The mRNA that was associated with hnRNP-E1 was immunoprecipitated using antibodies against hnRNP-E1. The amount of co-precipitated MBP mRNA was quantified by using qRT-PCR, and the relative level of mRNA, compared with that obtained by using control IgG antibody incubated with mRNA without hnRNP-E1, was calculated. Data show the mean±s.e.m. of four independent experiments. Statistical significance was analyzed by one-way ANOVA followed by Dunnett's multiple comparison test. *$P<0.05$; ***$P<0.001$; ns, non-significant.

data therefore suggest that the opposing effects of hnRNP-E1 and hnRNP-K result from competition for shared binding sites within the 3′-UTR of the MBP mRNA. No changes in the expression level of either hnRNP-E1 or hnRNP-K were observed during oligodendrocyte differentiation or at the onset of MBP translation. However, increased levels of hnRNP-K were found in granular-like structures outside the nucleus in MBP-positive cells but not in MBP-negative cells, suggesting that this change in the subcellular localization of hnRNP-K is associated with the initiation of translation of the MBP mRNA.

Based on these and previous experiments, we now propose a working hypothesis in which remodeling of the RNP particle occurs prior to the final stages of transport and is required for the initiation of translation (Fig. 8D). We suggest that, following nuclear export, the mRNP complex that contains the MBP mRNA also contains hnRNP-E1 and hnRNP-A2, and is mainly located in the cell body and primary processes. HnRNP-E1 is required to maintain the translational silencing of the mRNA at this stage, whereas hnRNP-A2 is required for the first step of transport into the processes. By contrast, hnRNP-K is recruited to the mRNA granules only at a later stage, requiring the release of hnRNP-E1 prior to binding. In this model, remodeling of the RNP particle, including exchange of hnRNP-E1 and hnRNP-K, is likely to be a prerequisite for the targeting of mRNA to the myelin sheath, or for the recruitment of protein factors required for the initiation of translation. Previous experiments suggest that the transport velocity of the RNA granules is altered at branch points of the primary processes before they enter the myelin sheet (Ainger et al., 1993). In addition, hnRNP-K knockdown leads to increased accumulation of MBP mRNA at process branch points (Laursen et al., 2011). Based on these observations, and on the fact that hnRNP-E1 is present principally within the cell body and primary processes, the process branch point might be the subcellular site where the proposed remodeling of the RNP particles occurs.

The ability of hnRNP-K and hnRNP-E1 to bind to the same elements in the 3′-UTR of a tightly regulated mRNA is similar to their known interaction with DICEs in the 3′-UTR of 15-lipoxygenase mRNA (Ostareck et al., 1997). The mRNA of 15-lipoxygenase is translated to produce an enzyme for which timely expression is essential to induce mitochondrial degradation at the time when reticulocytes become mature erythrocytes (Ostareck et al., 1997). However, in contrast to the opposing effects on translation in our system, both hnRNP-K and hnRNP-E1 inhibit translation of 15-lipoxygenase mRNA (Ostareck et al., 1997; Ostareck et al., 2001; Naarmann et al., 2008). Another difference between the two systems is that 15-lipoxygenase mRNA contains ten copies of the DICE element located next to one another, allowing simultaneous binding of hnRNP-K and hnRNP-E1 (Reimann et al., 2002). Here, we identify only two distantly located binding sites in the MBP 3′-UTR, and we demonstrate that these sites cannot support simultaneous binding of hnRNP-E1 and hnRNP-K, emphasizing different regulatory functions in these two systems.

It will be of particular interest to delineate the molecular mechanism controlling the exchange of hnRNP-E1 for hnRNP-K. RNP remodeling has been suggested to play an essential role in the regulation of mRNA fate (Lee and Lykke-Andersen, 2013). However, RNP remodeling during mRNA transport in the cytosol of *Xenopus* oocytes (Lewis et al., 2008) and prior to the translation of protamine 2 mRNA in mouse spermatids (Fukuda et al., 2013) are, to our knowledge, the only similar examples described so far. Interestingly, in the latter example, remodeling is suggested to involve competition between splice variants of CBF-A for binding to an RTS sequence. In oligodendrocytes, RNP remodeling has only been associated previously with nuclear export of the MBP mRNA, which has been shown to depend on the exchange of different splice variants of Quaking, an RNA-binding protein. Isoform 5 of Quaking causes retention of the MBP mRNA in the nucleus, whereas isoforms 6 or 7 are required for export. Disturbing the balance between the isoforms of Quaking, as observed in the quaking mouse, results in nuclear retention of the mRNA and lack of MBP expression (Larocque et al., 2002). The molecular mechanism that allows exchange of these factors is not known but, in other systems, remodeling of the RNP particles is tightly linked to helicase activity (Linder, 2008). Interestingly, recent experiments identified a helicase, DDX54, as being required for normal MBP expression (Zhan et al., 2013). However, whether this is involved in the remodeling of the RNP particle prior to nuclear export, in the translation of mRNA or in other processes remains to be studied.

Finally, we observed that the ability of the oligodendrocytes to extend their long branched processes and myelin sheets to cover a large surface area correlates with the timing of MBP synthesis. This was shown by knockdown of hnRNP-E1 and hnRNP-K, which caused decreased or increased cell size, respectively. A possible explanation for this is that lack of inhibitory hnRNP-E1 in the cell body results in accumulation of MBP protein, preventing further cell growth. By contrast, a reduction and delay in MBP protein synthesis, as observed upon hnRNP-K knockdown, allows further cell growth. This implies that temporal and spatial control of MBP protein synthesis imposed by the balance between hnRNP-E1 and hnRNP-K is crucial for normal myelination. Similarly, mutations in the motor protein Kif1b result in disrupted mRNA transport, causing accumulation of MBP protein in the cell body of

Journal of Cell Science (2014) 127, 1550–1564 doi:10.1242/jcs.140855

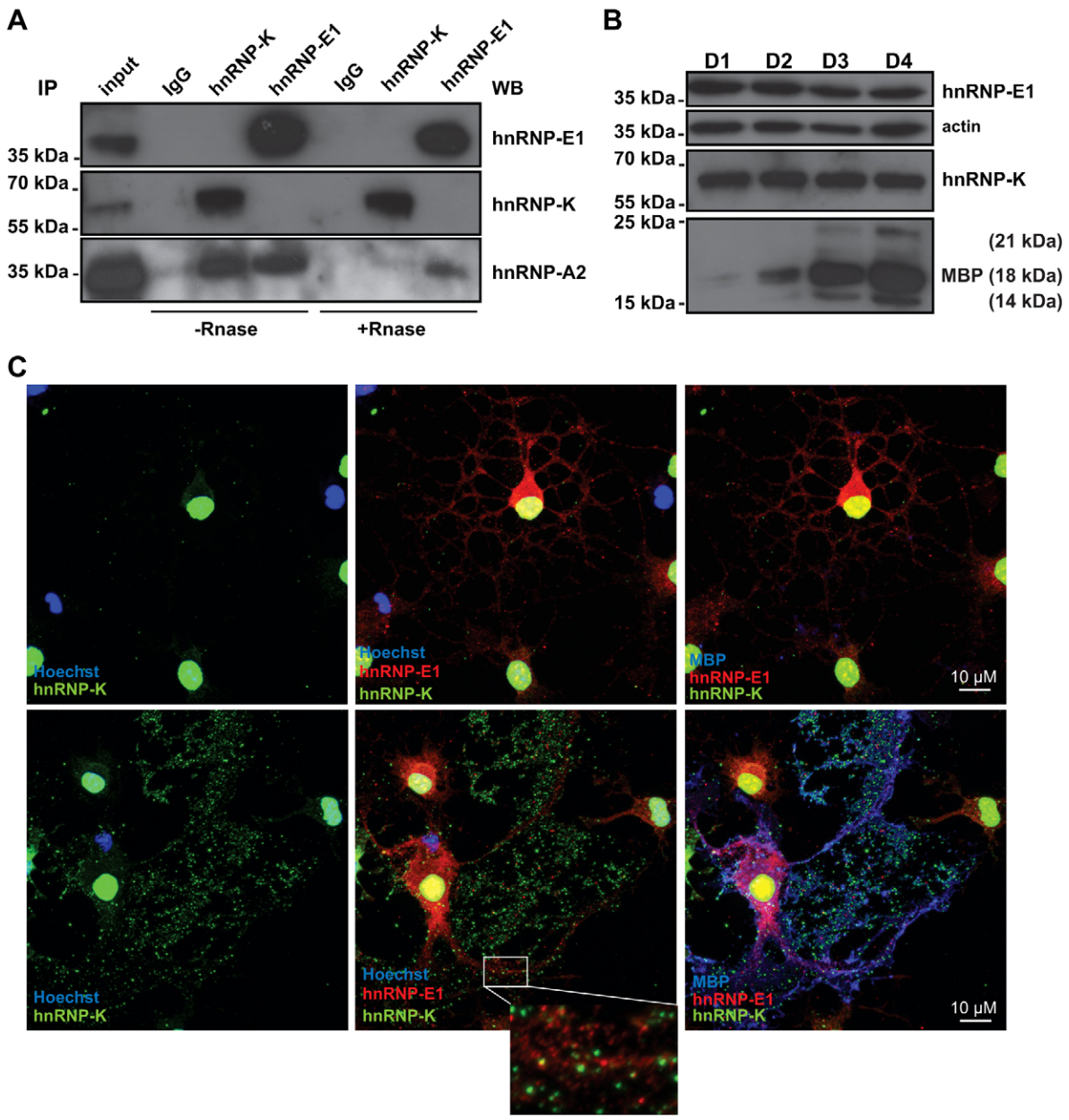

Fig. 6. hnRNP-K and hnRNP-E1 show different binding to hnRNP-A2 and distinct localization within differentiating oligodendrocytes.
(A) Immunoprecipitation from lysates of mature oligodendrocytes using control IgG, or antibodies against hnRNP-K or hnRNP-E1, followed by incubation with or without RNase. The precipitates were analyzed by western blotting for hnRNP-E1, hnRNP-K and hnRNP-A2, as indicated. Note that in the absence of RNase treatment, hnRNP-A2 co-precipitated with both hnRNP-K and hnRNP-E1. No co-precipitation of hnRNP-K with hnRNP-E1 was observed. Also note that RNase treatment abolished the co-precipitation of hnRNP-A2 with hnRNP-K, whereas co-precipitation of hnRNP-E1 and hnRNP-A2 was still evident in the RNase-treated samples. (B) Western blots of lysates of oligodendrocyte precursor cells cultured for 1–4 days were probed for hnRNP-E1, hnRNP-K and MBP. Actin was used as a loading control. Note that differentiation affects the expression level of MBP but not that of hnRNP-E1 or hnRNP-K. (C) Oligodendrocyte precursors differentiated for 3 days in culture were stained with antibodies against hnRNP-K (red), hnRNP-E1 (green) and MBP (blue), as indicated. A representative MBP-negative cell (upper panels) and MBP-positive cell (lower panels) is shown. Note that hnRNP-K is localized mainly in the nucleus of the MBP-negative cell, but is also present in granules of the developing myelin sheets in the MBP-positive cell. By contrast, hnRNP-E1 is present mainly in the cell body and primary processes of both MBP-negative and MBP-positive cells. The enlargement of the boxed region in the middle lower panel shows that hnRNP-K and hnRNP-E1 are not colocalized outside the nucleus. Of more than 5000 hnRNP-K-positive granules in 15 cells, less than 3% were found to also contain hnRNP-E1.

the oligodendrocytes and abnormal myelination (Lyons et al., 2009). The latter is interesting because the mutated Kif1b, which is likely to result in a general defect in cellular transport associated with microtubules, allows expression of MBP in the cell body. This is in contrast to what we observe following hnRNP-A2 knockdown, with lack of mRNA transport leading to decreased MBP expression. A possible explanation for this difference might be that the components causing release from transport particles and initiation of translation are not present in the cell body in a normal polarized oligodendrocyte. Thus, polarization of the oligodendrocyte and concomitant intracellular trafficking, induced by the interaction of the oligodendrocyte processes with axons, is likely to be a central mechanism to confine translational activation signals to this interface. The remodeling of

Journal of Cell Science (2014) 127, 1550–1564 doi:10.1242/jcs.140855

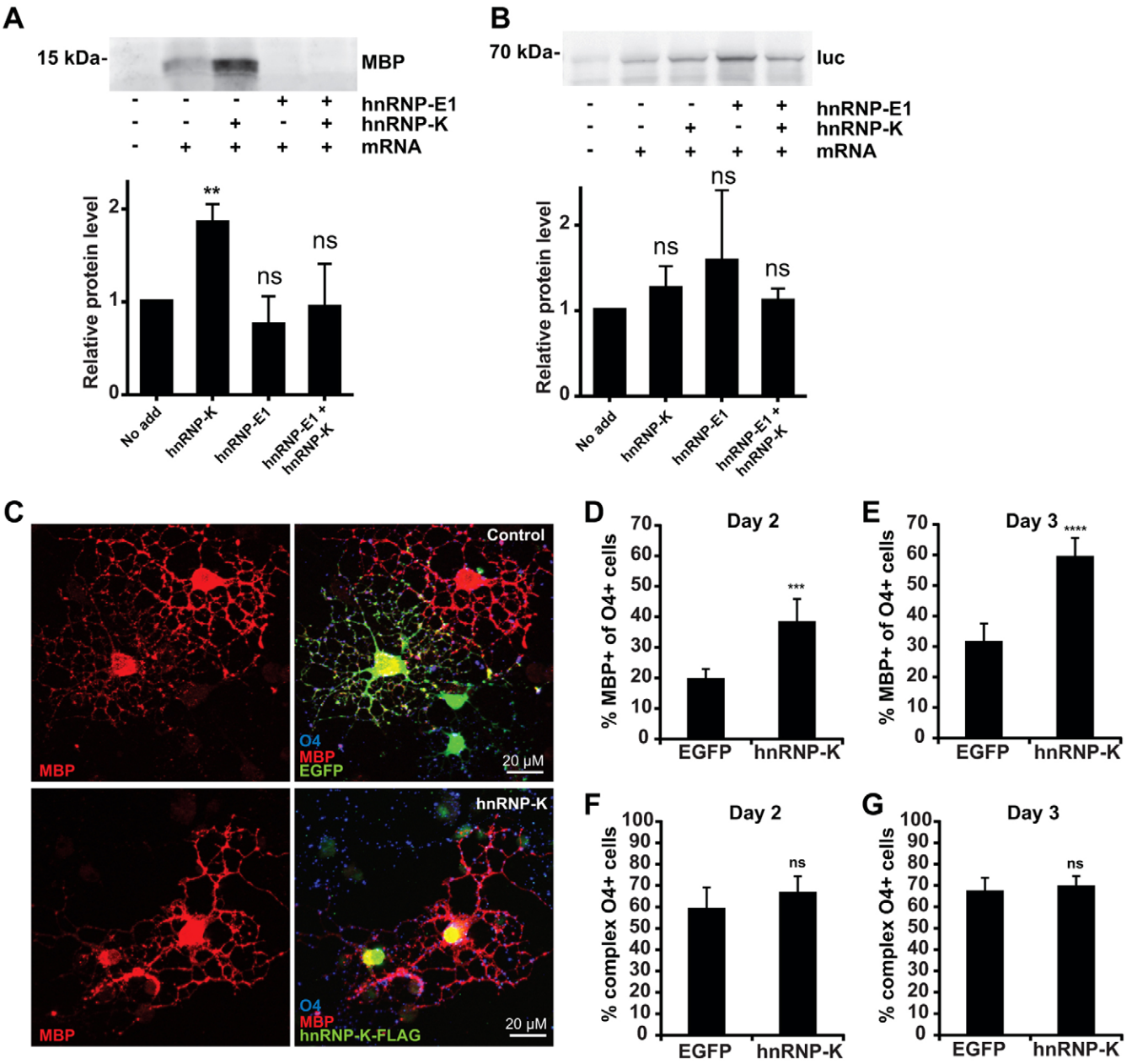

Fig. 7. hnRNP-K induces expression of MBP. (A) MBP mRNA (20 ng/μl), including the 3′-UTR, was *in vitro* translated using a rabbit reticulocyte lysate (RRL) in the absence or presence of hnRNP-K (0.15 μM), hnRNP-E1 (0.3 μM) or a combination thereof, as indicated. The amount of MBP synthesized was assessed by western blotting using MBP antibodies, and was quantified by densitometry. The data show the mean±s.d. of at least three independent experiments. Statistical significance was analyzed by one-way ANOVA followed by Dunnett's multiple comparision test. (B) A control experiment similar to A was performed using luciferase mRNA (20 ng/μl). (C) Immunocytochemistry of oligodendrocyte precursors that were transfected with EGFP (green) or hnRNP-K-FLAG (green), and stained 2 days after transfer to differentiation medium. The cells were also stained for MBP (red) and O4 (blue), a marker of maturing oligodendrocytes. The percentage of O4-positive cells that were positive for MBP at day 2 (D) and day 3 (E), and the percentage of oligodendrocytes showing complex branching morphology at day 2 (F) and day 3 (G) are shown. Data show the mean±s.d. of three independent experiments. Statistical significance was analyzed by Student's *t*-test. $^{**}P<0.01$; $^{***}P<0.001$; $^{****}P<0.0001$; ns, non-significant.

the RNP particle represents an additional regulatory layer allowing the temporal and spatial regulation of MBP mRNA translation.

MATERIALS AND METHODS

Plasmid construction and cloning

A reporter construct, pcDNA3.1-EGFP-3′-UTR, containing EGFP cDNA fused with the full-length 3′-UTR of MBP, was generated from pEGFP-3′-UTR (Laursen et al., 2011) using the *Xho*I and *Hind*III sites of pcDNA3.1 (Invitrogen). Truncated variants were then made by PCR, using the primer EGFP-Fw (5′-CGATCTCGAGATGGTGAGCAAGGGCGAGGA-3′) in combination with 640-Rev (5′-CAGTAAGCTTGAGTCGACCAAGGTACACGG-3′), 810-Rev (5′-CAGTAAGCTTGGAAGCCTGGACCACACAGT-3′), 963-Rev (5′-CAGTAAGCTTCTGGCCTGGAAGCGTCCCCAG-3′) or 1500-Rev (5′-CAGTAAGCTTAGTCAGTACGTTAGAGGGATG-3′). Nucleotide 1 is the first nucleotide of the coding sequence (nucleotide 78 of nm_017026). The RTS of the MBP 3′-UTR was deleted (-RTS) or mutated (A8G) by overlap-extension PCR (Ho et al., 1989). The outer primers were EGFP-Fw and EGFP-3′-UTR-Rev (5′-CAGTAAGCTTCAAAGATCATTGCAAGT-3′). The inner

Journal of Cell Science (2014) 127, 1550–1564 doi:10.1242/jcs.140855

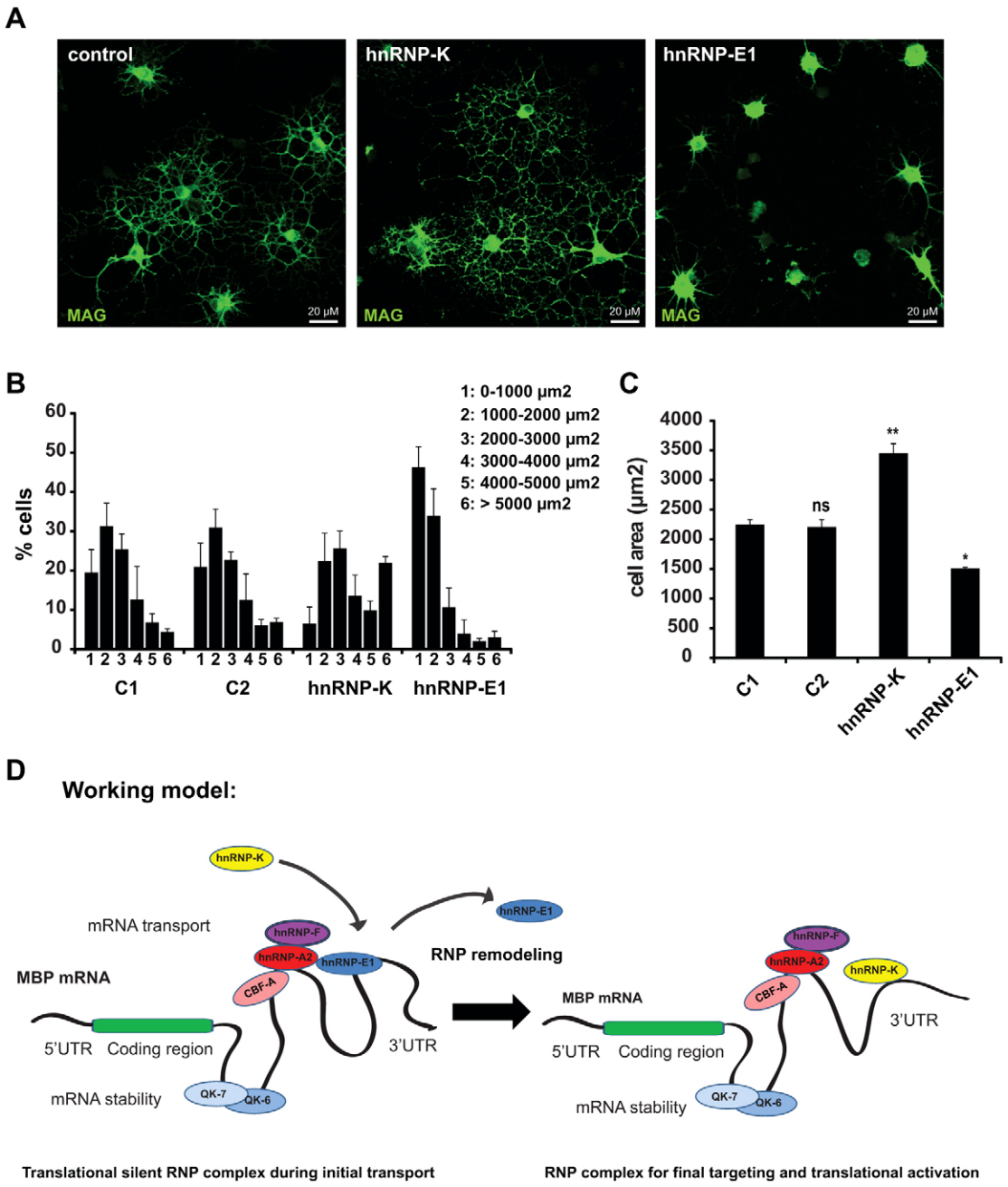

Fig. 8. Extension of oligodendrocyte processes is differentially regulated by hnRNP-K and hnRNP-E1 knockdown. (A) Immunocytochemistry for mature (MAG-positive) oligodendrocytes generated from oligodendrocyte precursors transfected with non-targeting siRNA (control), or siRNA targeting hnRNP-K or hnRNP-E1, as indicated. Note that knockdown of hnRNP-K increased cell size, whereas cell size was decreased by knockdown of hnRNP-E1. The size distribution (B) and average sizes (C) of the cells following siRNA treatment are shown. At least 200 cells at day 2.5 from three independent experiments were analyzed, and data show the mean±s.e.m. *$P<0.05$; **$P<0.01$; ns, non-significant; one-way ANOVA followed by Tukey's multiple comparison test. (D) A simplified working model. RNP remodeling is required for MBP mRNA translation. Based on our results, we suggest that the RNP particle containing the MBP mRNA undergoes remodeling in the oligodendrocyte processes prior to targeting to the myelin sheet and initiation of translation. We propose that during such remodeling, inhibitory hnRNP-E1 is exchanged with stimulatory hnRNP-K.

primers were -RTS-Fw (5′-AGGCACACCGCGCAGGGGACTGTG-TGGTCC-3′) and -RTS-Rev (5′-CCCCTGCGCGGTGTGCCTGTCT-ATCCGCAG-3′); and A8G-Rev (5′-CCATGCTCTCTGGCCCCTTGG-CGGTGTGCC-3′) and A8G-Fw (5′-GGCACACCGCCAAGGGGCCA-GAGAGCATGG-3′), respectively. The regions containing nucleotides 640–810 and 963–1500 were deleted or fused directly to EGFP cDNA by overlap-extension PCR. For +640–810, the outer primers were EGFP-Fw and 810-Rev, and the inner primers were +640–810-Fw (5′-GACTCAG-ATCTTGACCGGAGGTTCAGGTGCACGGAC-3′) and +640–810-Rev (5′-CCTGAACCTCCGGTCAAGATCTGAGTCCGGAC-3). For Δ640–810, the outer primers were EGFP-Fw and EGFP-3′-UTR-Rev, and the inner primers were Δ640–810-Fw (5′-GGTCGACTCTTTGTTTTCTT-TCCCC-3′) and Δ640–810-Rev (5′-GAAAACAAAGAGTCGACCAA-GGTACACGG-3′). For +963–1500, the outer primers were EGFP-Fw and 1500-Rev, and the inner primers were +963–1500-Fw (5′-TCCGGA-CTCAGATCTTGAGCGGTTCCCTGCACCCCACCAG-3′) and +963–1500-Rev (5′-GCAGGGAACCGCTCAAGATCTGAGTCCGGACTT-GTA-3′). For Δ964–1500, the outer primers were EGFP-Fw and

Journal of Cell Science (2014) 127, 1550–1564 doi:10.1242/jcs.140855

EGFP-3′-UTR-Rev, and the inner primers were Δ964–1500-Fw (5′-CCAGGCCAGATGTCTTTTGATTTAGCATGTC-3′) and Δ964–1500-Rev (5′-CAAAAGACATCTGGCCTGGAAGCGTCC-3′). The mutated fragments were cloned into the *Xho*I/*Hind*III sites of pcDNA 3.1. A control reporter construct, pcDNA3.1-EGFP, was generated with the primers EGFP-Fw and EGFP-Rev (5′-CAGTAAGCTTTTACTTGTACAGCTCGTCC-3′). The fragment was cloned into the *Xho*I/*Hind*III sites of pcDNA3.1. A cDNA fragment encoding hnRNP-E1 (XM_575592.3) was amplified from oligo-dT cDNA that was generated from mRNA isolated from rat oligodendrocytes, using the primers hnRNP-E1-Fw (5′-ATGCCTCGAGATGGACGCCGGTGTGACTGAAAG-3′) and hnRNP-E1-Rev (5′-ATGCAAGCTTGCTGCACCCCATGCCCTTCTCAGAGG-3′). The fragment was cloned into the *Hind*III/*Xho*I sites of pcDNA3.1-myc-HisA (Invitrogen) to generate pcDNA3.1-hnRNP-E1-myc-His. The plasmid pcDNA3.1-hnRNP-E1-FLAG was generated in parallel, using the primers hnRNP-E1-Fw and FLAG-hnRNP-E1-Rev (5′-ATGCAAGCTTCTACTTATCGTCGTCATCCTTGTAATCCTCGCTGCACCCCATGCCCTTCTCAGAGG-3′). Similarly, a cDNA fragment encoding hnRNP-K (BC061867.1) was amplified from oligo-dT cDNA that was generated from rat oligodendrocyte mRNA, using primers hnRNP-K-Fw (5′-GTAGCTCGAGATGGAGACCGAACAGCCAGA-3′) and hnRNP-K-Rev (5′-GTACGGATCCGAATCCTTCAACATCTGCATACTGC-3′). The fragment was cloned into the *BamH*I/*Xho*I sites of pcDNA3.1-myc-HisA to generate pcDNA3.1-hnRNP-K-myc-His. The plasmid pcDNA3.1-hnRNP-K-FLAG was generated similarly, using the primers hnRNP-K-Fw and FLAG-hnRNP-K-Rev (5′-GTAGGGATCCTTACTTGTCATCGTCATCCTTGTAATCGAATCCTTCAACATCTGCATACTGCTTCAC-3′).

Expression and purification of recombinant proteins

For recombinant expression of hnRNP-E1 and hnRNP-K, HEK293T cells cultured in DMEM with 10% fetal calf serum (FCS) and 1× penicillin-streptomycin were transfected with pcDNA3.1-hnRNP-K-myc-His or pcDNA3.1-hnRNP-E1-myc-His using the calcium phosphate precipitation method (Pear et al., 1993). At 48–72 hours post-transfection, the cells were lysed as described below. For hnRNP-K purification the soluble fractions were pooled and transferred to Ni-NTA Sepharose beads (GE Healthcare), and incubated for 2 hours at 4℃ with rotation. The beads were washed with PBS containing 0.5 M NaCl and 20 mM sodium phosphate pH 5.5, and with PBS. Elution was performed with PBS containing 50 mM EDTA. Peak fractions were pooled, diluted in buffer A (50 mM Tris-HCl pH 7.4, 50 mM KCl and 0.5 mM DTT) and loaded onto a Mono-Q FPLC column (GE Healthcare) equilibrated in buffer A. The column was eluted by a linear gradient formed from buffer A and a solution of 50 mM Tris-HCl pH 7.4, 500 mM KCl and 0.5 mM DTT. Fractions were pooled and dialyzed against PBS containing 0.5 mM DTT. For hnRNP-E1 purification, soluble fractions were loaded onto a HisTrap HP column (GE Healthcare). The column was washed with PBS containing 0.5 M NaCl, PBS containing 1 M NaCl, and PBS. Elution was performed with PBS containing 50 mM EDTA. Peak fractions were pooled, diluted in buffer B (50 mM Tris-HCl pH 8.5, 25 mM KCl and 0.5 mM DTT) and loaded onto a Mono-Q FPLC column (GE Healthcare) equilibrated in buffer B. The column was eluted by a linear gradient formed from buffer B and a solution of 50 mM Tris-HCl pH 8.5 and 500 mM KCl. HnRNP-E1 fractions were pooled, further purified on a Superose 12 column (GE Healthcare) equilibrated in PBS, concentrated and quantified.

Cell culture and transfection

Primary oligodendrocyte precursor cells (OPCs) were obtained as described previously (McCarthy and de Vellis, 1980). The OPCs were cultivated in Sato medium (Bottenstein and Sato, 1979) supplemented with 0.5% FCS, PDGF (10 ng/ml) and FGF (10 ng/ml). Transfection of the OPCs with plasmids was performed by using FuGENE 6 (Promega). The day after transfection, cells were trypsinized and re-plated onto poly-D-lysine-coated coverslips in 12-well plates. Cells were allowed to differentiate in Sato medium supplemented with 0.5% FCS and 1× penicillin-streptomycin. Transfection of OPCs with siRNA was carried out as described previously (Laursen et al., 2011). The sequences of the siRNA duplexes used for knockdown of hnRNP-K were: 5′-AAAGGUGGUCAGCGGAUUA-3′, 5′-CGACAGAAGAGGACGGCCU-3′, 5′-GUGCUGAUAUUGAGACGAU-3′ and 5′-CCGAUAGGGUUGUAGAAUG-3′. The sequences for hnRNP-A2 knockdown were 5′-GAUGAGAGCCCAGAGGUAA-3′, 5′-GAGCAUCACCUUAGAGAUU-3′, 5′-GGAAAUUAUGGAAGUGGAA-3′ and 5′-GCGGGAUCCUGCAAGCAAA-3′. The sequences for hnRNP-E1 knockdown were 5′-CCGCUAAGAAUUUAAAGAA-3′, 5′-AGAAAGGGGAGUCGGUGAA-3′, 5′-CCAAAUAACUUAAUCGGCU-3′ and 5′-AGUGUAGGUUCGCUCGUAA-3′. For controls, an 'ON-TARGET plus' non-targeting pool of duplexes was used. All siRNA species were from Dharmacon (Thermo Scientific). Oli-neu cells, an oligodendrocyte precursor cell line (Jung et al., 1995), were cultured in Sato medium supplemented with 1% horse serum, at 37℃ under 5% CO_2. Culture under these conditions for up to 3 days does not induce endogenous expression of MBP in these cells (Trajkovic et al., 2006; Laursen et al., 2011). In addition, the Oli-neu cells express hnRNP-A2, hnRNP-E1 and hnRNP-K at levels comparable to primary oligodendrocytes (supplementary material Fig. S1A). Transfection of Oli-neu cells was carried out as described previously (Laursen et al., 2011).

Translation assay

Oli-neu cells were co-transfected with pcDNA3.1-EGFP, pcDNA3.1-EGFP-3′-UTR-MBP, or mutated variants thereof, and pDsRed-Express (Clontech). At 48 hours post-transfection, the cells were detached with trypsin, washed with cold DMEM containing 2% FCS, spun down and resuspended in PBS with 2% paraformaldehyde (PFA), and analyzed on a Beckman Coulter FC 500 MPL. For each experiment, at least 25×10^3 cells were analyzed. The translation ratio was calculated as the mean level of green fluorescence divided by the mean level of red fluorescence. The relative expression of the different EGFP constructs was calculated as the translation ratio divided by the translation ratio for cells transfected with pcDNA3.1-EGFP and pDsRed-Express. Total RNA was purified from a fraction of the transfected cells with the RNeasy Mini Kit (Qiagen), and the levels of EGFP and actin mRNA were assessed by RT-PCR using the OneStep RT-PCR Kit (Qiagen), with the following primers: EGFP-RT-Fw 5′-TATATCATGGCCGACAAGCA-3′, EGFP-RT-Rev 5′-GAACTCCAGCAGGACCATGT-3′, actin-RT-Fw 5′-AGCCATGTACGTAGCCATCC-3′ and actin-RT-Rev 5′-CTCTCAGCTGTGGTGGTGAA-3′.

Immunocytochemistry and microscopy

Cells were fixed with 4% PFA, blocked with PBS containing 10% goat serum and 0.1% Triton-X 100 for 1 hour, and incubated with primary antibodies diluted in blocking buffer for 2 hours. After washing with PBS, the cells were incubated with secondary antibodies diluted in blocking buffer for 1 hour, washed with PBS and mounted with Fluoromount-G (SouthernBiotech). Antibodies against hnRNP-K, hnRNP-E1 and the FLAG tag were from Sigma, antibody against EGFP was from Life Technologies, antibodies against MBP and O4 were from Serotec and antibody against MAG was from Millipore. All secondary antibodies were from Invitrogen. Hoechst 33342 nuclear stain (Invitrogen) was included in the final washing buffer. Images were acquired by using a Zeiss Axiovert LSM 510 confocal microscope or a Zeiss Axio Observer.Z1 Apotome 2 microscope. Image analysis was performed using ImageJ and Photoshop.

Western blotting and protein analysis

Cells were washed in ice-cold PBS and lysed in 1% Triton X-100, 10 mM Tris-HCl pH 7.4, 5 mM EDTA, 150 mM NaCl, with proteinase and phosphatase inhibitors for 15 minutes on ice. The cells were scraped off and transferred into microtubes. The lysates were centrifuged at 4℃. Proteins were separated by SDS-PAGE and blotted onto PVDF membrane (Millipore). The membranes were dried and blocked in 2% Tween-20, followed by overnight incubation with primary antibodies in TBS-T (20 mM Tris-HCl pH 7.6 and 150 mM NaCl, containing 0.1% Tween-20). Membranes were washed in TBS-T and incubated for 1 hour

with horseradish peroxidase (HRP)-conjugated secondary antibodies (GE Healthcare), washed again in TBS-T, and developed using ECL-Plus (GE Healthcare). Images were acquired on X-ray films (Konica-Minolta).

Immunoprecipitation

Lysates were prepared as described above with the addition of RNase inhibitors in the lysis buffer. The lysates were incubated with antibodies cross-linked to protein G beads (GE Healthcare) at 4℃ for 4 hours, followed by four successive washes in lysis buffer, and then dissolved in SDS sample buffer. The antibodies used were anti-hnRNP-K (Sigma), anti-hnRNP-E1 (Sigma) or control IgG (Jackson Laboratories). Cross-linking was carried out as described previously (Laursen et al., 2011).

RNA-immunoprecipitation

Oligodendrocytes (2.5×10^6) were lysed in the presence of RNase inhibitors as above, and RNA was isolated as described previously (Peritz et al., 2006; Laursen et al., 2011). The precipitated RNA was spun down, resuspended in 20 µl of H_2O and subjected to DNase treatment for 10 minutes at room temperature prior to purification using the RNeasy MinElute Cleanup Kit (Qiagen), with elution in 15 µl of H_2O. The RNA was reverse transcribed and amplified with Brilliant III Ultra-Fast SYBR Green QRT-PCR (Stratagene), and analyzed on a Stratagene Mx3005P. The following Q-PCR primers were used: MBP, 5′-ACT-TGGCCACGCAAACTACC-3′ and 5′-GGGTGTACGAGGTGTCAC-AA-3′; PLP, 5′-TGTTTGGGAAAATGGCTAGG-3′ and 5′-AGCA-TTCCATGGGAGAACAC-3′; G6PDH, 5′-GCAAACAGAGTGAGCC-CTTC-3′ and 5′-CATAGGAGTTACGGGCAAAGA-3′. The relative enrichment of PLP and MBP mRNA to G6PDH was calculated as described previously (Bauer et al., 2012).

RNA-competition assay

MBP mRNA (0.8 µg) containing the 3′-UTR generated by *in vitro* transcription using the mMessage mMachine Kit (Ambion) was preincubated with 1 µg of purified recombinant hnRNP-E1 for 30 minutes, followed by the addition of 3 or 7.5 µg of purified recombinant hnRNP-K. RNA associated with hnRNP-E1 was then isolated by RNA-immunoprecipitation as described above. RNA binding to non-specific IgG beads without the addition of proteins was used as a negative control. Finally, the amount of mRNA associated with hnRNP-E1 with and without the addition of hnRNP-K was assessed by QRT-PCR as detailed above, and the enrichment of MBP mRNA relative to the negative control was calculated.

Electrophoretic mobility shift assay (EMSA)

DNA templates for the synthesis of RNA probes were generated by PCR, using pcDNA3.1-MBP-3′-UTR (Laursen et al., 2011) as a template and specific primers as detailed in supplementary material Table S1. The RNA probes were synthesized by *in vitro* transcription using the MAXIScript T7 RNA Polymerase Kit (Applied Biosystems), followed by biotinylation using the Pierce RNA 3′ End Biotinylation Kit (Thermo Scientific). EMSA analysis was carried out using the LightShift Chemiluminescent RNA EMSA Kit (Thermo Scientific). The standard reaction mixture was supplemented with 5% glycerol, 5 mM $MgCl_2$ and 0.1 mg/ml tRNA. For each binding reaction, 2.5 pmol of biotinylated RNA and 0.2–1.5 µg of recombinantly expressed protein (see above) was used.

In vitro translation

In vitro transcribed full-length MBP mRNA or luciferase RNA (20 ng/µl) was translated using the Flexi RRL kit (Promega). Purified recombinant hnRNP-K (0.15 µM) and/or hnRNP-E1 (0.3 µM) was added to the reaction mixture. The reaction mixtures were analyzed by using western blotting with antibodies against MBP or luciferase. Images were captured by using an ImageQuant LAS 4000 (GE Healthcare) instrument and quantified.

Competing interests

The authors declare no competing interests.

Author contributions

J.T.J. and L.S.L. designed the experiments. J.T.J., J.S., L.R., L.B.F. and L.S.L. performed the experiments. J.T.J. and L.S.L. analyzed the data, and L.S.L. wrote the manuscript with input from J.T.J.

Funding

This work was supported by the Lundbeck Foundation [grant number R44-A4083]; the Novo Nordic Foundation [grant number R179-A15546]; the Carlsberg Foundation [grant number 2011_01_0289/40]; and the Danish MS Society [grant number R192-A9287].

Supplementary material

Supplementary material available online at
http://jcs.biologists.org/lookup/suppl/doi:10.1242/jcs.140855/-/DC1

References

Aggarwal, S., Yurlova, L., Snaidero, N., Reetz, C., Frey, S., Zimmermann, J., Pähler, G., Janshoff, A., Friedrichs, J., Müller, D. J. et al. (2011). A size barrier limits protein diffusion at the cell surface to generate lipid-rich myelin-membrane sheets. *Dev. Cell* **21**, 445-456.

Aggarwal, S., Snaidero, N., Pähler, G., Frey, S., Sánchez, P., Zweckstetter, M., Janshoff, A., Schneider, A., Weil, M. T., Schaap, I. A. et al. (2013). Myelin membrane assembly is driven by a phase transition of myelin basic proteins into a cohesive protein meshwork. *PLoS Biol.* **11**, e1001577.

Ainger, K., Avossa, D., Morgan, F., Hill, S. J., Barry, C., Barbarese, E. and Carson, J. H. (1993). Transport and localization of exogenous myelin basic protein mRNA microinjected into oligodendrocytes. *J. Cell Biol.* **123**, 431-441.

Ainger, K., Avossa, D., Diana, A. S., Barry, C., Barbarese, E. and Carson, J. H. (1997). Transport and localization elements in myelin basic protein mRNA. *J. Cell Biol.* **138**, 1077-1087.

Backe, P. H., Messias, A. C., Ravelli, R. B., Sattler, M. and Cusack, S. (2005). X-ray crystallographic and NMR studies of the third KH domain of hnRNP K in complex with single-stranded nucleic acids. *Structure* **13**, 1055-1067.

Bauer, N. M., Moos, C., van Horssen, J., Witte, M., van der Valk, P., Altenhein, B., Luhmann, H. J. and White, R. (2012). Myelin basic protein synthesis is regulated by small non-coding RNA 715. *EMBO Rep.* **13**, 827-834.

Bottenstein, J. E. and Sato, G. H. (1979). Growth of a rat neuroblastoma cell line in serum-free supplemented medium. *Proc. Natl. Acad. Sci. USA* **76**, 514-517.

Colman, D. R., Kreibich, G., Frey, A. B. and Sabatini, D. D. (1982). Synthesis and incorporation of myelin polypeptides into CNS myelin. *J. Cell Biol.* **95**, 598-608.

Colognato, H., Ramachandrappa, S., Olsen, I. M. and ffrench-Constant, C. (2004). Integrins direct Src family kinases to regulate distinct phases of oligodendrocyte development. *J. Cell Biol.* **167**, 365-375.

Dejgaard, K. and Leffers, H. (1996). Characterisation of the nucleic-acid-binding activity of KH domains. Different properties of different domains. *Eur. J. Biochem.* **241**, 425-431.

Fukuda, N., Fukuda, T., Sinnamon, J., Hernandez-Hernandez, A., Izadi, M., Raju, C. S., Czaplinski, K. and Percipalle, P. (2013). The transacting factor CBF-A/Hnrnpab binds to the A2RE/RTS element of protamine 2 mRNA and contributes to its translational regulation during mouse spermatogenesis. *PLoS Genet.* **9**, e1003858.

Gebauer, F., Preiss, T. and Hentze, M. W. (2012). From cis-regulatory elements to complex RNPs and back. *Cold Spring Harb. Perspect. Biol.* **4**, a012245.

Ho, S. N., Hunt, H. D., Horton, R. M., Pullen, J. K. and Pease, L. R. (1989). Site-directed mutagenesis by overlap extension using the polymerase chain reaction. *Gene* **77**, 51-59.

Hoek, K. S., Kidd, G. J., Carson, J. H. and Smith, R. (1998). hnRNP A2 selectively binds the cytoplasmic transport sequence of myelin basic protein mRNA. *Biochemistry* **37**, 7021-7029.

Holcik, M. and Liebhaber, S. A. (1997). Four highly stable eukaryotic mRNAs assemble 3′ untranslated region RNA-protein complexes sharing cis and trans components. *Proc. Natl. Acad. Sci. USA* **94**, 2410-2414.

Jung, M., Krämer, E., Grzenkowski, M., Tang, K., Blakemore, W., Aguzzi, A., Khazaie, K., Chlichlia, K., von Blankenfeld, G., Kettenmann, H. et al. (1995). Lines of murine oligodendroglial precursor cells immortalized by an activated neu tyrosine kinase show distinct degrees of interaction with axons in vitro and in vivo. *Eur. J. Neurosci.* **7**, 1245-1265.

Kosturko, L. D., Maggipinto, M. J., D'Sa, C., Carson, J. H. and Barbarese, E. (2005). The microtubule-associated protein tumor overexpressed gene binds to the RNA trafficking protein heterogeneous nuclear ribonucleoprotein A2. *Mol. Biol. Cell* **16**, 1938-1947.

Kosturko, L. D., Maggipinto, M. J., Korza, G., Lee, J. W., Carson, J. H. and Barbarese, E. (2006). Heterogeneous nuclear ribonucleoprotein (hnRNP) E1 binds to hnRNP A2 and inhibits translation of A2 response element mRNAs. *Mol. Biol. Cell* **17**, 3521-3533.

Kwon, S., Barbarese, E. and Carson, J. H. (1999). The cis-acting RNA trafficking signal from myelin basic protein mRNA and its cognate trans-acting ligand hnRNP A2 enhance cap-dependent translation. *J. Cell Biol.* **147**, 247-256.

Larocque, D., Pilotte, J., Chen, T., Cloutier, F., Massie, B., Pedraza, L., Couture, R., Lasko, P., Almazan, G. and Richard, S. (2002). Nuclear retention of MBP mRNAs in the quaking viable mice. *Neuron* **36**, 815-829.

Laursen, L. S., Chan, C. W. and ffrench-Constant, C. (2009). An integrin-contactin complex regulates CNS myelination by differential Fyn phosphorylation. *J. Neurosci.* **29**, 9174-9185.
Laursen, L. S., Chan, C. W. and ffrench-Constant, C. (2011). Translation of myelin basic protein mRNA in oligodendrocytes is regulated by integrin activation and hnRNP-K. *J. Cell Biol.* **192**, 797-811.
Lee, S. R. and Lykke-Andersen, J. (2013). Emerging roles for ribonucleoprotein modification and remodeling in controlling RNA fate. *Trends Cell Biol.* **23**, 504-510.
Lewis, R. A., Gagnon, J. A. and Mowry, K. L. (2008). PTB/hnRNP I is required for RNP remodeling during RNA localization in Xenopus oocytes. *Mol. Cell. Biol.* **28**, 678-686.
Linder, P. (2008). mRNA export: RNP remodeling by DEAD-box proteins. *Curr. Biol.* **18**, R297-R299.
Lyons, D. A., Naylor, S. G., Scholze, A. and Talbot, W. S. (2009). Kif1b is essential for mRNA localization in oligodendrocytes and development of myelinated axons. *Nat. Genet.* **41**, 854-858.
McCarthy, K. D. and de Vellis, J. (1980). Preparation of separate astroglial and oligodendroglial cell cultures from rat cerebral tissue. *J. Cell Biol.* **85**, 890-902.
Min, Y., Kristiansen, K., Boggs, J. M., Husted, C., Zasadzinski, J. A. and Israelachvili, J. (2009). Interaction forces and adhesion of supported myelin lipid bilayers modulated by myelin basic protein. *Proc. Natl. Acad. Sci. USA* **106**, 3154-3159.
Munro, T. P., Magee, R. J., Kidd, G. J., Carson, J. H., Barbarese, E., Smith, L. M. and Smith, R. (1999). Mutational analysis of a heterogeneous nuclear ribonucleoprotein A2 response element for RNA trafficking. *J. Biol. Chem.* **274**, 34389-34395.
Naarmann, I. S., Harnisch, C., Flach, N., Kremmer, E., Kühn, H., Ostareck, D. H. and Ostareck-Lederer, A. (2008). mRNA silencing in human erythroid cell maturation: heterogeneous nuclear ribonucleoprotein K controls the expression of its regulator c-Src. *J. Biol. Chem.* **283**, 18461-18472.
Ostareck, D. H., Ostareck-Lederer, A., Wilm, M., Thiele, B. J., Mann, M. and Hentze, M. W. (1997). mRNA silencing in erythroid differentiation: hnRNP K and hnRNP E1 regulate 15-lipoxygenase translation from the 3′ end. *Cell* **89**, 597-606.
Ostareck, D. H., Ostareck-Lederer, A., Shatsky, I. N. and Hentze, M. W. (2001). Lipoxygenase mRNA silencing in erythroid differentiation: The 3′UTR regulatory complex controls 60S ribosomal subunit joining. *Cell* **104**, 281-290.
Pear, W. S., Nolan, G. P., Scott, M. L., Baltimore, D. (1993). Production of high-titer helper-free retroviruses by transient transfection. *Proc Natl Acad Sci U S A* **90**, 8392-8396.
Peritz, T., Zeng, F., Kannanayakal, T. J., Kilk, K., Eiríksdóttir, E., Langel, U. and Eberwine, J. (2006). Immunoprecipitation of mRNA-protein complexes. *Nat. Protoc.* **1**, 577-580.
Pratt, C. A. and Mowry, K. L. (2013). Taking a cellular road-trip: mRNA transport and anchoring. *Curr. Opin. Cell Biol.* **25**, 99-106.
Raju, C. S., Göritz, C., Nord, Y., Hermanson, O., López-Iglesias, C., Visa, N., Castelo-Branco, G. and Percipalle, P. (2008). In cultured oligodendrocytes the A/B-type hnRNP CBF-A accompanies MBP mRNA bound to mRNA trafficking sequences. *Mol. Biol. Cell* **19**, 3008-3019.
Readhead, C., Popko, B., Takahashi, N., Shine, H. D., Saavedra, R. A., Sidman, R. L. and Hood, L. (1987). Expression of a myelin basic protein gene in transgenic shiverer mice: correction of the dysmyelinating phenotype. *Cell* **48**, 703-712.
Reimann, I., Huth, A., Thiele, H. and Thiele, B. J. (2002). Suppression of 15-lipoxygenase synthesis by hnRNP E1 is dependent on repetitive nature of LOX mRNA 3′-UTR control element DICE. *J. Mol. Biol.* **315**, 965-974.
St Johnston, D. (2005). Moving messages: the intracellular localization of mRNAs. *Nat. Rev. Mol. Cell Biol.* **6**, 363-375.
Thisted, T., Lyakhov, D. L. and Liebhaber, S. A. (2001). Optimized RNA targets of two closely related triple KH domain proteins, heterogeneous nuclear ribonucleoprotein K and alphaCP-2KL, suggest Distinct modes of RNA recognition. *J. Biol. Chem.* **276**, 17484-17496.
Trajkovic, K., Dhaunchak, A. S., Goncalves, J. T., Wenzel, D., Schneider, A., Bunt, G., Nave, K. A. and Simons, M. (2006). Neuron to glia signaling triggers myelin membrane exocytosis from endosomal storage sites. *J. Cell Biol.* **172**, 937-948.
Trapp, B. D., Moench, T., Pulley, M., Barbosa, E., Tennekoon, G. and Griffin, J. (1987). Spatial segregation of mRNA encoding myelin-specific proteins. *Proc. Natl. Acad. Sci. USA* **84**, 7773-7777.
Wake, H., Lee, P. R. and Fields, R. D. (2011). Control of local protein synthesis and initial events in myelination by action potentials. *Science* **333**, 1647-1651.
White, R., Gonsior, C., Krämer-Albers, E. M., Stöhr, N., Hüttelmaier, S. and Trotter, J. (2008). Activation of oligodendroglial Fyn kinase enhances translation of mRNAs transported in hnRNP A2-dependent RNA granules. *J. Cell Biol.* **181**, 579-586.
White, R., Gonsior, C., Bauer, N. M., Kraemer-Albers, E. M., Luhmann, H. J. and Trotter, J. (2012). HnRNP F is a novel component of oligodendroglial RNA transport granules contributing to the regulation of MBP protein synthesis. *J. Biol. Chem.* **287**, 1742-1754.
Xing, L. and Bassell, G. J. (2013). mRNA localization: an orchestration of assembly, traffic and synthesis. *Traffic* **14**, 2-14.
Yoga, Y. M., Traore, D. A., Sidiqi, M., Szeto, C., Pendini, N. R., Barker, A., Leedman, P. J., Wilce, J. A. and Wilce, M. C. (2012). Contribution of the first K-homology domain of poly(C)-binding protein 1 to its affinity and specificity for C-rich oligonucleotides. *Nucleic Acids Res.* **40**, 5101-5114.
Zhan, R., Yamamoto, M., Ueki, T., Yoshioka, N., Tanaka, K., Morisaki, H., Seiwa, C., Yamamoto, Y., Kawano, H., Tsuruo, Y. et al. (2013). A DEAD-box RNA helicase Ddx54 protein in oligodendrocytes is indispensable for myelination in the central nervous system. *J. Neurosci. Res.* **91**, 335-348.